

REPORT DOCUMENTATION PAGE

1a. REPORT SECURITY CLASSIFICATION <b>UNCLASSIFIED</b>		1b. RESTRICTIVE MARKINGS <b>(2)</b>		
<b>AD-A181 017</b>		3. DISTRIBUTION/AVAILABILITY OF REPORT Approved For Public Release Distribution Unlimited		
		5. MONITORING ORGANIZATION REPORT NUMBER(S) <b>AFOSR-TM- 87-0742</b>		
6a. NAME OF PERFORMING ORGANIZATION Cornell University	6b. OFFICE SYMBOL (If applicable)	7a. NAME OF MONITORING ORGANIZATION AFOSR		
6c. ADDRESS (City, State and ZIP Code) Clark Hall Ithaca, NY 14853		7b. ADDRESS (City, State and ZIP Code) Bldg 410 Bolling AFB, DC 20332-6448		
8a. NAME OF FUNDING/SPONSORING ORGANIZATION AFOSR	8b. OFFICE SYMBOL (If applicable) NE	9. PROCUREMENT INSTRUMENT IDENTIFICATION NUMBER AFOSR-84-0314		
8c. ADDRESS (City, State and ZIP Code) Bldg 410 Bolling AFB, DC 20332-6448		10. SOURCE OF FUNDING NOS.		
		PROGRAM ELEMENT NO. 61102F	PROJECT NO. 2306	TASK NO. B2
11. TITLE (Include Security Classification) <b>Wavelength Independent Optical Microscopy &amp; Lithography</b>				
12. PERSONAL AUTHOR(S) Dr. A Lewis				
13a. TYPE OF REPORT Annual	13b. TIME COVERED FROM <u>Sept 84</u> TO <u>Sept 86</u>	14. DATE OF REPORT (Yr., Mo., Day) April 29, 1987	15. PAGE COUNT 17	
16. SUPPLEMENTARY NOTATION				
17. COSATI CODES		18. SUBJECT TERMS (Continue on reverse if necessary and identify by block number)		
FIELD	GROUP			SUB. GR.
19. ABSTRACT (Continue on reverse if necessary and identify by block number) In summary, our experiments thus far have demonstrated the feasibility of the subwavelength optical technology we have pioneered under this contract. Thus, these experiments confirm the exciting potential for applications of the near-field technology in a variety of areas of interest to the Air Force.				
20. DISTRIBUTION/AVAILABILITY OF ABSTRACT UNCLASSIFIED/UNLIMITED <input checked="" type="checkbox"/> SAME AS RPT. <input type="checkbox"/> DTIC USERS <input type="checkbox"/>		21. ABSTRACT SECURITY CLASSIFICATION UNCLASSIFIED		
22a. NAME OF RESPONSIBLE INDIVIDUAL KEVIN J MALLOY		22b. TELEPHONE NUMBER (Include Area Code) (202) 767-4933	22c. OFFICE SYMBOL NE	

DTIC  
ELECTE  
JUN 08 1987  
S D

**Best  
Available  
Copy**

**AFOSR-TR- 87 - 0742**

Progress Report

on

Wavelength Independent Optical Microscopy  
and Lithography [Grant #AFOSR-84-0314]

Submitted by:

M. Isaacson and A. Lewis  
Cornell University  
School of Applied and Engineering Physics  
Clark Hall  
Ithaca, New York 14853

Submitted to:

United States Air Force  
Office of Scientific Research

Covering the Period:

September, 1984 - September, 1986



Accession For	
NTIS CRA&I	<input checked="" type="checkbox"/>
DTIC TAB	<input type="checkbox"/>
Unannounced	<input type="checkbox"/>
Justification	
By .....	
Distribution /	
Availability Codes	
Dist	Avail and/or Special
A-1	

## PROGRESS REPORT

With the help of the Air Force we have been able to develop a new area of optics which is based on the collimation of near-field radiation. The near-field allows super spatial resolution for the characterization and fabrication of materials.

### CONCEPTUAL BASIS OF NEAR-FIELD SCANNING OPTICAL MICROSCOPY

At the start of the present contract we had only a rudimentary understanding of the nature of the near-field. As a result of this contract, great progress has been made both in building a theoretical foundation and underpinning this foundation with crucial experiments. The fundamental principle underlying the NSOM concept is outlined in Figure 1, where visible light is depicted as being normally incident on a conducting screen containing a small (sub-wavelength) aperture. Because the screen is completely opaque, the radiation emanating through the aperture and into the region beyond the screen is first collimated to the aperture size rather than to the wavelength of the radiation employed. This occurs in the near-field regime. Eventually the effect of diffraction is evidenced as a marked divergence in the radiation, resulting in a pattern that no longer reproduces the geometrical image of the aperture. This occurs in the far-field regime.

To apply the collimation phenomena, an object, such as an integrated circuit, is placed within the near-field region relative to an aperture. In this case, the aperture acts as a light source whose size is not limited by the considerations of geometrical optics. The light source can be scanned relative to the object, and the detected light can be used to generate a high-resolution image. Because the resolution is dependent upon the aperture size rather than the wavelength, it is possible to obtain resolution of  $<50\text{nm}$ , which is comparable to scanning electron microscopes, if sufficiently small apertures are used. These are the essential features of the NSOM technique, which, unlike electron microscopic methods, can be applied in air using non-ionizing visible radiation and can form images of fluorescing objects with this same degree of super-resolution.

### HISTORICAL BACKGROUND

As far back as a decade ago, the principle of super-resolution microscopy was demonstrated at microwave frequencies using a wavelength of 3cm by Ash and Nicholls (1). In their pioneering experiment, a grating of 0.5mm periodicity was imaged with an effective resolution of 1/60 the wavelength. However, until we reported our initial results in 1984 (2), there were no published attempts to extend this technique to the visible region of the spectrum. This is quite understandable, because the minute physical dimensions of the optical near-field demand aperture fabrication and micropositioning technologies on a nanometer scale. Furthermore, it is not immediately obvious that the results of the microwave experiment could be extended to the visible regime, because in the optical regime, thin metal films with finite conductivity had to be used to construct subwavelength apertures whereas in the microwave case comparatively thicker metal screens with infinite conductivity could be used. These questions together with the inability of the microwave microscope to scan rough surfaces led to little interest in the field.

However, since our original reports (2), several additional publications in the area of near-field imaging have appeared. Fischer (3) in West Germany has produced an interesting series of results by scanning a subwavelength aperture over a second, larger aperture, but these results were difficult to interpret for a number of reasons. For example, the opacity of the metal film used was not large so that the aperture was poorly defined and much stray light was transmitted through the aperture screens. In addition, because of the grazing incidence illumination in his experiment, a series of standing waves were generated when the polarization of the electric field was perpendicular to these screens.

Durig, et al. (4) in Zurich produced apertures at the tip of a single crystal of quartz etched using HF to make a fine point and covered this by metal. These apertures were difficult to produce reproducibly and to characterize because they were manufactured by thrusting this metal covered pyramidal quartz crystal against glass slide and detecting the first instant when light emanated from the aperture. Furthermore, these workers had difficulty in making test structures to demonstrate <50nm resolution. With any new form of microscopy it is essential to have test structures well-characterized by an established technique in order to verify the claim of subwavelength capability.

In short, initial attempts to implement the near-field scanning concept attest to the difficulty of the NSOM technique. To appreciate the technical challenges inherent in this form of microscopy, we completed detailed calculations under this contract to obtain a first approximation for how the radiation spreads out as it emanates from a subwavelength aperture. These calculations (5) and others completed on this contract (6,7) investigate the transmission of light through slits and apertures in screens of finite thickness.

In particular, the component of the time-averaged Poynting vector perpendicular to the screen was calculated in the region just beyond the screen. The results are shown in Figure 2, where the divergence of the energy flux is plotted as a function of the distance from the aperture. These results indicate that the radiation remains collimated to a distance of approximately the aperture diameter. Finally, the near-field energy flux calculations exhibit a close-to-exponential decrease in intensity with increasing distance from the screen. This suggests that rigid stability requirements are required for the z direction even for rough surfaces.

## OVERCOMING THE TECHNICAL CHALLENGES

### Aperture Fabrication

Several different methods have been used in the past to fabricate the submicron apertures needed in near-field microscopy (2-4). However, under this contract we developed an inexpensive, rapid, and highly reproducible method for producing such apertures at the tips of metallized glass pipettes. Besides the ease, rapidity, cheapness and reproducibility of our new technique an important advantage of our method is that these apertures at the tip of highly tapered pipettes can probe even recessed regions of rough surfaces. To form such apertures with diameters ranging from 50nm to 1000nm from glass micropipettes a two stage pulling process was used. Scanning electron

micrographs of a 100nm diameter pipette and a 500nm diameter pipette are compared in Figure 3. These pipettes were metallized with 8nm of chromium followed by 50nm of aluminum. The chromium was used as an adhesive layer between the glass pipette and the 50nm aluminum layer. Aluminum was chosen for its high absorption coefficient at optical wavelengths.

Our early attempts at forming these pipette apertures produced tip outer diameters of approximately 500nm for the smaller aperture pipettes. However, recently we have produced tips with outer diameters of 60nm, see Figure 4, using techniques used by biologists to produce pipettes for the microinjection of individual cells (8). We have discovered that we can make even smaller diameter pipettes with apertures at the tips by using aluminumsilicate instead of borosilicate glass. And we are now trying to optimize this new form of light wave technology.

Our application of these pipette type apertures to near-field microscopy and our demonstration (9) of large light throughputs from such apertures has resolved one of the principal problems in scanning rough, real surfaces with this form of super-resolution microscopy.

#### Micropositioning

Another major problem overcome during this contract year has been the development of a methodology to position an aperture 50nm above a surface with the 3nm accuracy required by the exponential behavior of the near-field. The placement of the aperture at the tip of a pipette certainly simplifies the problem but there has to be a feedback mechanism that will allow for the accurate positioning of the aperture above the surface. We have developed three distinct solutions to this problem all of which work well at resolving this potential barrier to near-field microscopy.

One method for distance regulation is based on an exquisitely sensitive technique for monitoring z topography developed by Matey and Blanc (10). In this technique the sample and a probe tip form a capacitor and changes in separation between the sample and the probe result in changes in capacitance. The capacitance changes can be detected with a high Q RLC circuit. We have modified the technique in two ways. First, we employ our metal coated pipette aperture instead of the stylus probe of an RCA videoplayer used by these previous workers. Second, position modulation of the probe is used. Thus we have incorporated essentially an electrical heterodyning method. With this modulation the detected signal has components at different frequencies and this permits the decoupling of the dielectric information from the topographic information. With such position modulation the technique should be sensitive to changes of less than  $10^{-18}$  farads. The advantages of this technique for z position regulation in near-field microscopy are three fold. First, because of its sensitivity, the capacitive method can respond quickly even to very small topographical changes and this allows for rapid (kHz) near-field scanning. Second, with position modulation it is possible to generate a signal which depends solely on topography and not on material properties (i.e. dielectric properties) of the surface. Third, for the probe size that we use, the capacitance changes can be detected from as far as 50nm from the surface.

In the eventuality that the sample is not conducting the light emanating from a subwavelength aperture in an opaque screen decreases exponentially with distance from the screen (5). Hence, in a reflection mode, the intensity of the light reflected back through the aperture is strongly dependent upon the aperture-sample separation and can be used to form a distance regulation system. In this method position modulation can also be employed to extract topographical information.

Finally, Durig, et al. (4) have employed the new methodology of tunneling microscopy (11) to accurately measure the z position of the aperture. However with tunneling microscopy the probe has to approach within 2 nm of the surface and this is at least an order of magnitude closer than is required for NSOM.

#### Vibration, acoustic and thermal isolation

In a typical laboratory environment, building vibrations exist at frequencies as low as 2-4Hz, although most of the vibrational energy is in the 5-30Hz range (12). In our environment, we have measured displacements of up to one micron in this frequency range. If this energy were to be transferred without attenuation to the critical components of an NSOM system, and if the aperture and object were not held together with sufficient rigidity, then their relative displacement could vary by two to three orders of magnitude greater than the precision required. To preclude this possibility, it is necessary to design an isolation system which attenuates both horizontal and vertical vibrations from the floor at frequencies above a few hertz. In addition, such a system must use a damping mechanism to insure that any vibrations transmitted to the microscope are transient in nature. This damping mechanism is also needed to reduce the vibrations induced by the motion of the sample stage itself in the course of a scan. Finally, an effective isolation system must also shield the NSOM instrument from acoustic vibrations, which fall in the 20Hz to 20kHz range. The isolation system designed under this contract and described in the next section accomplishes all of these objectives.

Although the thermal expansion coefficients of the various components of a NSOM system will vary widely with composition and size, we have found that the components expand/contract roughly 0.1-1.0 micron for every one degree centigrade increase/decrease in temperature. Hence, the differential rate of expansion of the aperture relative to an object has to be surmounted. This obstacle has been overcome by using two lines of attack. First, the entire instrument has been designed to insure that the thermal expansion of the aperture relative to the object is rather small and second, the apparatus is enveloped in a shell that protects against thermal fluctuations.

#### OVERVIEW OF A PROTOTYPE NSOM

In this section we describe a prototype NSOM instrument built under the present contract in our laboratory. For this description we will use a series of pictures taken during the building of the instrument. Shown in Figure 5 is the vibration isolation system on which the microscope was built. As can be seen it is a passive, dual stage isolation system composed of an optical table and a second stage air table on which the base of the microscope sits. On this base (see Figure 6) rests the sample stage which consists of motorized translators for coarse adjustment and the fine adjustment stage designed by

Wye Creek Instruments. This permits accurate xy positioning with a resolution of  $<5\text{nm}$ . The sample assembly which permits illumination from the bottom through the rectangular opening seen in the photograph, is surrounded by a stainless steel chamber lined with material for acoustic isolation (see Figure 7). As seen in Figure 8, a conventional optical microscope sits in the side opening of the steel shell and this permits viewing of the pipette as it is translated, with motorized and piezoelectric translators, toward the sample through the opening in the center of the cover. This circular design with the pipette in the center insures that the thermal expansion of the aperture relative to sample is small. Finally, an overview of the microscope is seen in Figure 9. In this overview we clearly see the magnets that we use for eddy current damping of vibrations induced by movements on the stage. These magnets surround the base of the microscope and emanate from pillars that rest on the optical table. The photomultiplier/detection system (not seen in the photograph) that monitors the light emanating from the back end of the pipette is placed on top of the center of the stainless steel shell that surrounds the sample chamber and this signal is recorded, for each position of the sample under the pipette, by one of two IBM PC AT computers. These computers control the scan, collect the data from both the capacitance and NSOM signals and perform the imaging tasks required.

#### RESULTS FROM THE CORNELL NSOM

In this section we will demonstrate that even in a fluorescence mode the resolution we have obtained with our instrument is comparable to the resolution obtained with scanning electron microscopes. To demonstrate this resolution we made test structures by contact printing a pattern from a mask formed by electron beam lithography. This mask of silicon nitride was placed in contact with a clear glass coverslip and the material to be deposited was then evaporated through the mask and onto the coverslip. For the transmission scans, 50nm of chromium was evaporated whereas 50nm of 3,4,9,10-perylene-tetracarboxylic dianhydride was used for the fluorescence measurements. The samples were then coated with 5nm of chromium to assure conductivity over the edge or grating. The patterns thus formed had sharp, well-characterized features as demonstrated by scanning electron microscopy, SEM. Such test patterns are essential to quantitatively assess the resolution of NSOM in both the transmission and fluorescence modes.

Figure 10 shows a transmission scan over a chromium step for both a 600nm and 100nm diameter aperture. The distance from 12% to 88% transmission scales with aperture size. In Figure 11 the high resolution NSOM data is compared to a linescan from an electron micrograph of the same edge. The SEM trace is a convolution of the edge profile with the beam profile and the secondary electron emission yield function. The edge profile can be estimated from the micrograph trace to have a width of 30nm assuming a beam diameter of 20nm. This finite width is a result of the contact printing process. The 12%-88% point in intensity of the NSOM trace is 60nm. This is the near-field beam profile convoluted with the 30nm edge width.

Using these results we can make quantitative comparisons between the SEM and both experimental and theoretical NSOM scans. The theoretical curve through the NSOM data in Figure 11 was generated by assuming exponential absorption in the chromium step and an intensity transmitted to the detector scaling as the third power of the unoccluded area as suggested by Bethe (13).

Also shown in Figure 11 is a conventional far-field optical line scan obtained from the edge using the same 0.55 NA objective lens as used for focusing the light for the NSOM scans. The solid line passing through these experimental points has been calculated from the theory for a conventional incoherent scanning optical microscope (14). The result of a similar calculation for a 1.4NA objective is shown at the top of Figure 11. Thus, one can infer that resolution far exceeding the diffraction limit has been achieved using near-field scanning techniques and this emphasizes the exciting potential of being able to form subwavelength light spots for characterization and fabrication.

Using the same pipettes as were used for the data above we have obtained scans of fluorescent edges and gratings. One such scan of a fluorescent grating of period 800nm is shown in Figure 12A. A densitometer trace of a scanning electron micrograph of the same perylene grating is also shown in Figure 12B. The sharpest maximum and minimum change in the fluorescence NSOM image is <50nm. Thus fluorescence NSOM grating scans have been demonstrated with resolution comparable to the aperture diameter used and comparable to scanning electron micrographs of the same grating. The resolution obtained (15) is at least an order of magnitude better than the emission wavelength which is at 700nm.

#### WAVELENGTH INDEPENDENT LITHOGRAPHY

Considerable progress has also been made in the development of the necessary experimental methodology to produce the lithographic resists that are necessary for subwavelength lithography. The most successful method uses a Langmuir-Blodgett trough which can produce with high accuracy and reproducibility thicknesses down to a few nanometers. We have shown under this contract that pinhole free layers of such resists can be produced (16). For our initial experiments we used Shipley AZ 1400-5 resist which we were able to spin on as layers of less than 50nm. The scheme we used to impress various patterns on this resist is illustrated in Figure 13A. We developed a combination of a point mount and vacuum suction to bring the substrate into close contact with a quartz mask that was produced by contact printing with aluminum or chrome. Figure 13B shows what is seen when the mask and substrate are viewed from the top. Essentially the black central circle is the region that is within the near-field. The dimensionality of the various components in this scheme is shown in cross-section in Figure 13C. The method of fabrication of the quartz mask is seen in Figure 14. In this figure the pattern which is produced by electron beam lithography is further etched into silicon nitride via reactive ion etching. This mask is used to produce the contact print on quartz. The contact printing process is depicted in Figure 15. As can be seen Cr or Al is thermally evaporated through the silicon nitride mask onto the quartz plate. A scanning electron micrograph of a typical metal on quartz mask is shown in Figure 16. The resulting optical lithograph in the near-field is shown in Figure 17. As can be seen the grating is faithfully reproduced in silicon to better than 200nm resolution using light of 450nm. We expect to get much better resolution once the fabrication quality of our masks is improved with the recently installed electron beam machine at the National Submicron Research and Resource Facility.

In summary, our experiments thus far have demonstrated the feasibility of the subwavelength optical technology we have pioneered under this contract. Thus, these experiments confirm the exciting potential for applications of the near-field technology in a variety of areas of interest to the Air Force.

## REFERENCES

1. Ash, E.A. and Nicholls, G., *Nature (Lond.)* 237, 510 (1972).
2. Lewis, A., Isaacson, M., Harootunian, A., and Muray, A., *Ultramicroscopy* 13, 227 (1984).
3. Fisher, U. Ch., *J. Vac. Sci. Technol. B.* 3, 1498 (1985).
4. Durig, U., Pohl, D.W., and Rohner, F., *J. Appl. Phys.* 59, 3318 (1986).
5. Betzig, E., Harootunian, A., Lewis, A., and Isaacson, M., *Appl. Opt.* 25, 1890 (1986).
6. Leviatan, Y., *J. Appl. Phys.* 60, 1577 (1986).
7. Harootunian, A., *Near-Field Scanning Optical Microscopy and Raman Microscopy*, Cornell University Ph.D. Dissertation (1986).
8. Brown, K.T., and Flaming, D.G., *Neuroscience* 2, 813 (1977).
9. Betzig, E., Lewis, A., Harootunian, A., Isaacson, M., and Kratschmer, E., *Biophys. J.* 49, 269 (1986).
10. Matey, J.R., and Blanc, J., *J. Appl. Phys.* 57, 1437 (1985).
11. Binning, G., and Rohner, H., *Helvetica Physica Acta* 55, 726 (1982).
12. Newport Research Corporation Catalog 1983-84, Vol. 13, Fountain Valley, CA.
13. Bethe, H.A., *Phys. Rev.* 66, 163 (1944).
14. Wilson, T., and Shepard, C., *Theory and Practice of Scanning Optical Microscopy*, (Academic Press Inc., London 1984), p. 34.
15. Harootunian, A., Betzig, E., Isaacson, M., and Lewis, A., *Appl. Phys. Lett.* 49, 674 (1986).
16. Schildkraut, J. and Lewis, A., *Thin Solid Films* 134, 13 (1986).

FIGURE CAPTIONS

Figure 1: Schematic representation showing the collimation of radiation emanating from a subwavelength aperture.

Figure 2: The energy flux emanating from a 50nm diameter aperture normalized to the energy of the incident plane wave, is shown plotted as a function of both the perpendicular distance ( $z$ ) from an 180nm thick conducting screen and the ratio of the lateral distance from the center of the aperture to the half width of the aperture ( $x/a$ ). Notice that the radiation is collimated to roughly the edge of the aperture ( $x/a = 1$ ) out to  $z=60$ nm.

Figure 3: Scanning electron micrographs of metallized pipettes with aperture of diameters 100nm and 500nm at the tips of the pipettes.

Figure 4: Scanning electron micrograph of a 50nm outer diameter pipette.

Figure 5: Shown is the passive vibration isolation system used. Part of the air table used is seen at the bottom of the picture. On this air table is a second stage isolation air table which was home-built and on top of this is placed a Newport surface which serves as the base of the microscope.

Figure 6: Place on the microscope base is the coarse adjustment, motorized translators on which sits a piezoelectric nanometer scanning stage. In the center of this stage sits a circular glass coverslip on which the sample rests. The rectangular opening in the front of the coarse  $xy$  stages is for illumination of the sample from the bottom. This is accomplished by a mirror and a long working distance lens that is installed in the stage and focusses the light through the glass coverslip on which the sample sits.

Figure 7: Surrounding the  $xy$  stages seen in Fig. 6 is a stainless steel shell that also sits on the microscope base. Lining this shell is material for acoustic shielding.

Figure 8: A stainless steel cover is bolted to the stainless steel shell seen in Fig. 7. In the center of this cover is the opening into which the pipette with the coarse  $z$  translator and fine adjustment  $z$  piezoelectric fits. In the side of the shell is the microscope which allows the pipette to be viewed as it is brought into proximity of the sample. Also in view at the bottom left hand side of the picture are the optics for the inverted microscope that allows viewing the sample from the bottom as it is translated under the pipette by the coarse stage. Notice that the design decouples the  $xy$  motion from the  $z$  motion. Thus as the sample is rapidly scanned under the pipette the  $z$  piezoelectric, in response to one of the feedback mechanisms described in the text, independently adjusts the  $z$  position of the pipette aperture relative to the sample surface so that a constant sample/aperture separation is maintained. Notice also that the circular design minimizes thermal drift problems.

Figure 9: An overview of the NSOM instrument is seen in this figure. Surrounding the instrument are posts that are bolted to the optical table. Each of these posts have magnets that protrude into copper blocks that sit on the base of the microscope. These magnet/copper block assemblies are for eddy

current damping of vibrations that arise from the motions of the microscope during a scan. Seen in the background is the material that forms the walls of the room that surround the microscope. This material provides acoustic isolation. In fact everything except the microscope sits outside this acoustic enclosure. This includes the laser and the two IBM PC AT computers that control the microscope, collect the data and form the images with a special board and a high resolution dedicated graphics system from Imaging Technology. Also seen in the upper right of the picture is the erector set that holds the photomultiplier and detection system. The photomultiplier is placed just above the opening in the stainless steel plate that fits over the stainless steel shell. In this position the photomultiplier can detect the photons that emanate from the back end of the pipette as the sample is translated rapidly under the aperture. Thus, at each position of the sample the photons detected by the photomultiplier are recorded into the memory of one of the two computers and subsequently, within 2secs. after a scan an image appears on the Imaging Technology monitor. This NSOM image can be overlaid with the z topography capacitance image which is available at the same time.

Figure 10: Bottom low resolution (aperture=600nm) and top high resolution (aperture=100nm) transmission NSOM scans of a 50nm chromium edge are shown above. Wavelength used was 570nm.

Figure 11: NSOM and SEM comparisons. From bottom to top are shown: a densitometer trace of a scanning electron micrograph of a 50nm thick chromium edge; an NSOM scan of the same edge using 570nm excitation plotted against a theoretical NSOM curve; a theoretical scanning optical microscope (SOM) scan (570nm excitation and NA=0.55) plotted with points from an experimental optical micrograph scan of the same 50nm thick chrome step taken with 570nm excitation and the NA=0.55 optics used for focusing the light on the grating for the NSOM scans; and a theoretical SOM edge scan using a very high (1.4 NA) numerical aperture objective and 570nm excitation. All edge scan steps were normalized to an intensity change of unity.

Figure 12: A fluorescent NSOM and SEM comparison. A fluorescence NSOM scan of a perylene grating with a period of 800nm (A) is shown below a densitometer trace of a SEM scan of the same grating (B). The SEM scan was slightly displaced in a direction parallel to the grating lines relative to the NSOM scan.

Figure 13: A) Schematic of our method of optical pattern transfer B) Top view seen in optical microscope when contact is made between resist and mask C) Cross-sectional view of the optical pattern transfer method.

Figure 14: Method of printing mask fabrication.

Figure 15: Schematic of quartz contact printing.

Figure 16: Scanning electron micrograph of fabricated quartz mask.

Figure 17: A scanning electron micrograph of a near-field replication of a sub-500nm periodicity grating.

PAPERS PUBLISHED UNDER THIS CONTRACT

1. E. Betzig, A. Lewis, A. Harootunian, M. Isaacson and E. Kratschmer, "Near-Field Scanning Optical Microscopy (NSOM)," *Biophys. J.* 49, 269 (1986).
2. E. Betzig, A. Harootunian, A. Lewis and M. Isaacson, "Near Field Diffraction by a Slit: Implications for Super-Resolution Microscopy," *Appl. Optics*, 25, 1896 (1986).
3. A. Harootunian, E. Betzig, M. Isaacson, and A. Lewis, "Super-Resolution Fluorescence Near Field Scanning Optical Microscopy," *Appl. Phys. Lett.* 49, 674 (1986).
4. M. Isaacson, E. Betzig, A. Harootunian and A. Lewis, "Scanning Optical Microscopy at  $\lambda/10$  Resolution Using Near Field Imaging Methods" in "Recent Advances in Electron and Light Imaging in Biology and Medicine" *Annals of the New York Academy of Sciences*, Vol. 483, p. 448 (1986).
5. A. Lewis, E. Betzig, A. Harootunian, M. Isaacson and E. Kratschmer, "Near-Field Imaging of Fluorescence," in Spectroscopic Membrane Probes, ed. Leslie M. Loew (CRC press, 1986).
6. Y. Leviatin, "Study of Near Zone Fields of a Small Aperture," *Journal of Appl. Phys.* 60, 1577 (1986).

Ph.D. THESIS

1. A. Harootunian, "Near Field Scanning Optical Microscopy and Raman Microscopy" Ph.D. Thesis, Cornell University, January, 1986.

INVITED LECTURES CONCERNING THE RESEARCH SUPPORTED BY THIS CONTRACT  
(SEPT. 1984 - SEPT. 1986).

1. September 1984: Reichart-American Optical Corporation Laboratory, Buffalo, New York. "Near Field Scanning Optical Microscopy", M. Isaacson
2. February 1985: Biophysical Society Meeting, Baltimore, Maryland. "Near Field Scanning Optical Microscopy", A. Lewis
3. March 1986: New York Academy of Sciences, New York City. "Near Field Scanning Optical Imaging", M. Isaacson
4. June 1986: Whitney Symposium on Science and Technology. GE Research and Development Laboratory, Schenectady, New York. "Near Field Optical Imaging" M. Isaacson
5. August 1986: Microbeam Analysis Society Meeting, Albuquerque, New Mexico. "Near Field Scanning Optical Microscopy and Lithography", M. Isaacson
6. September 1986: Tohoku University, Sendai, Japan. "Optical Microscopy at 500Å Resolution", M. Isaacson

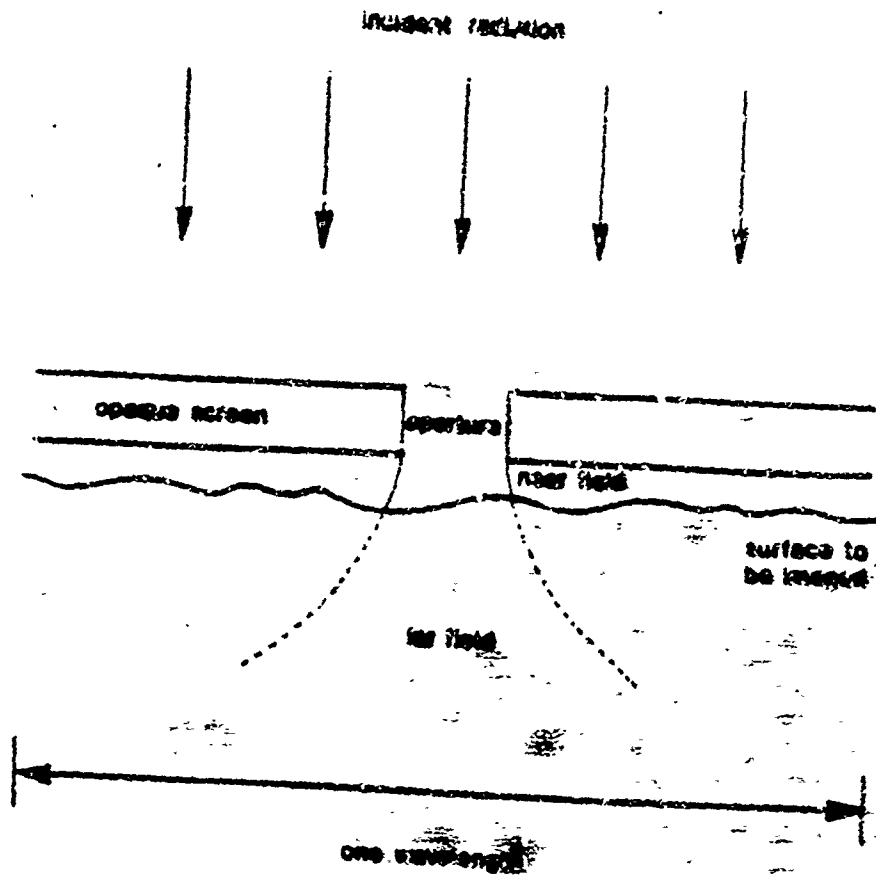


Figure 1

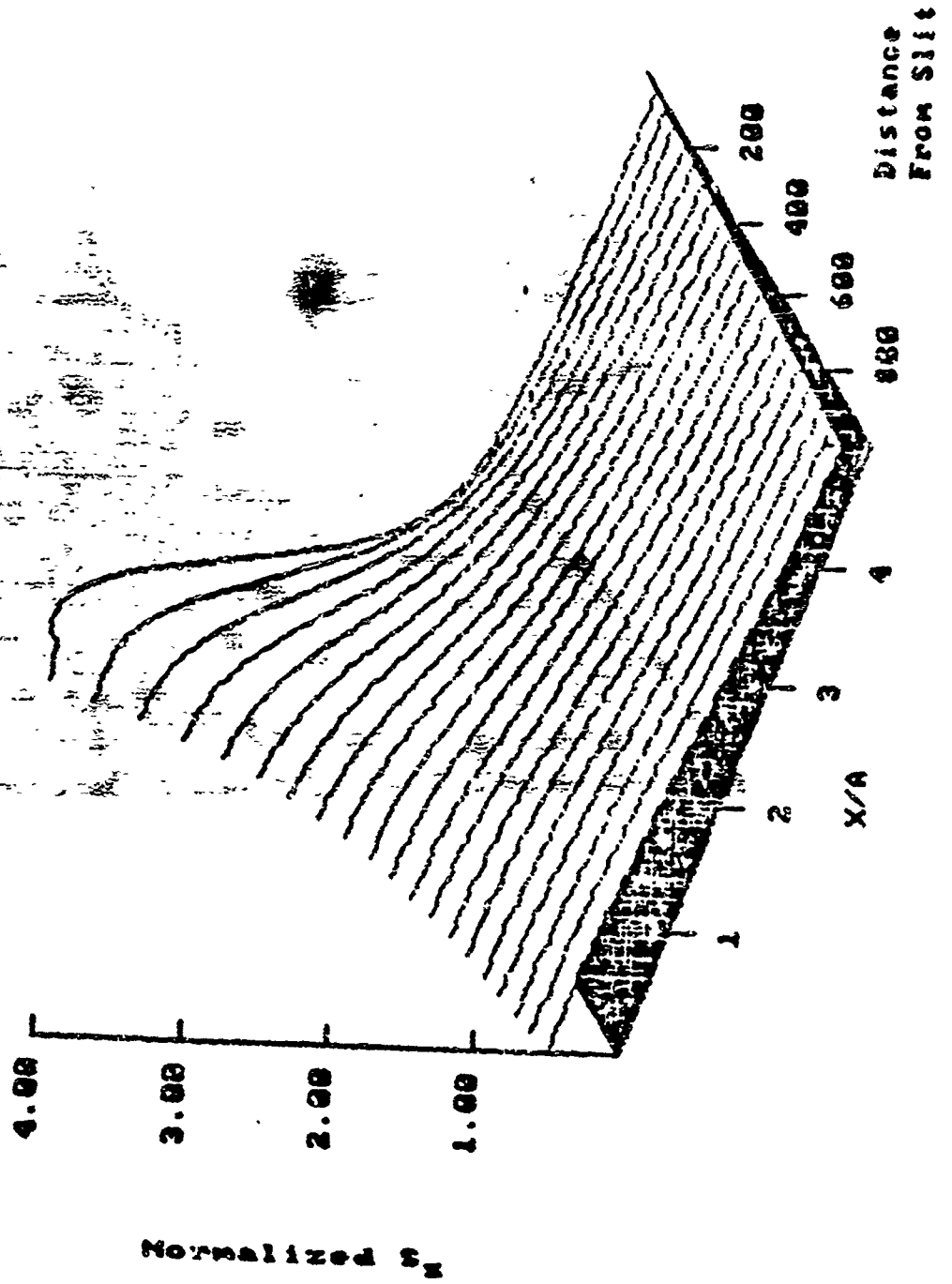


Figure 2



Figure 3

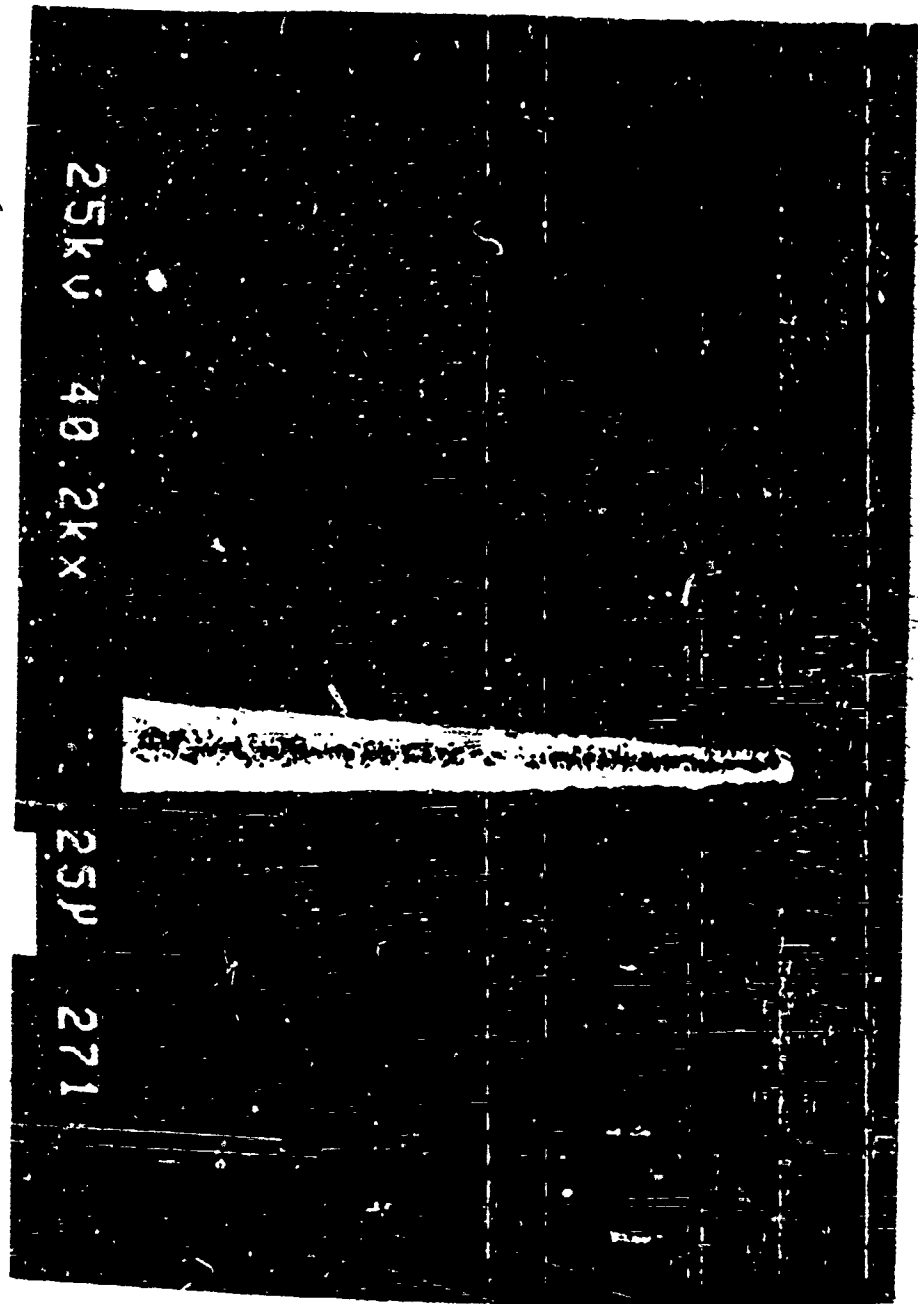


Figure 4

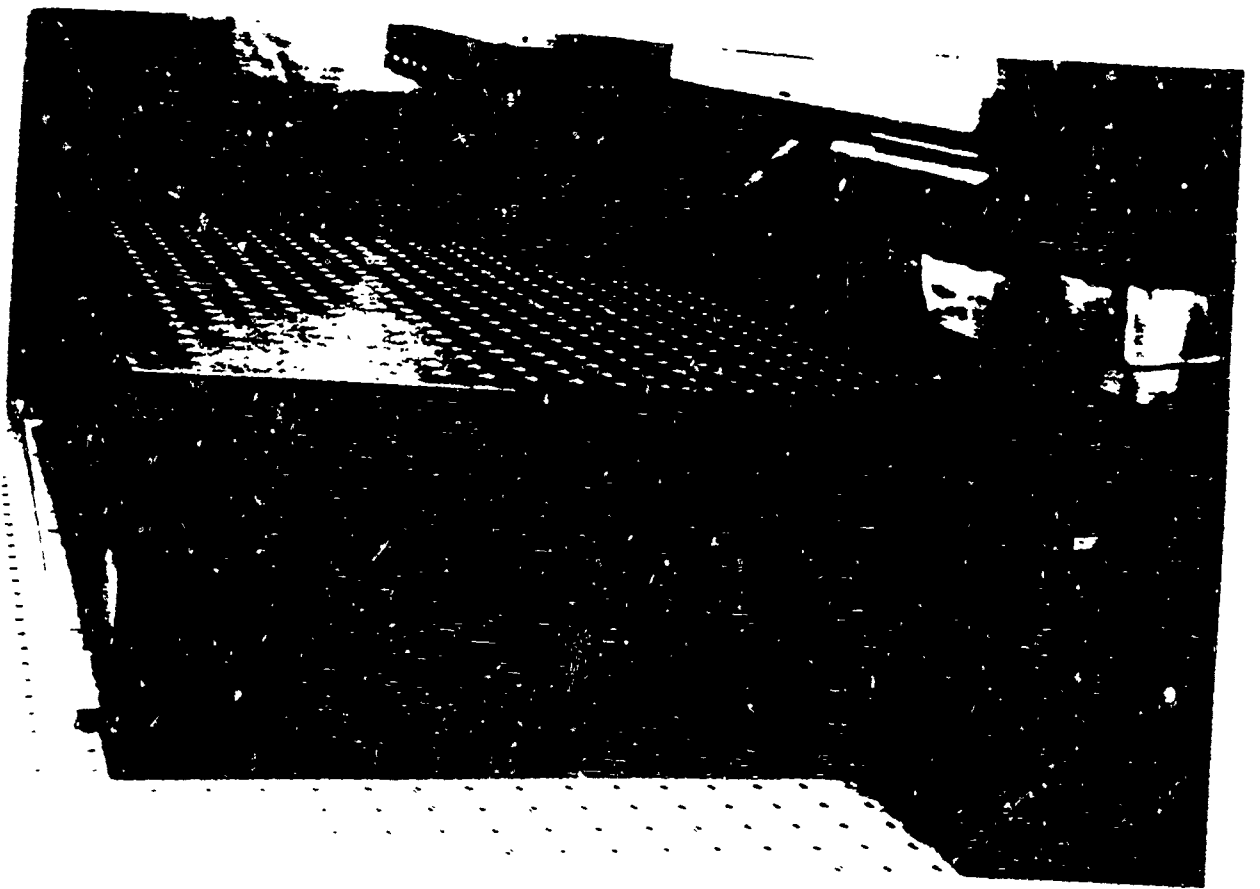


Figure 5

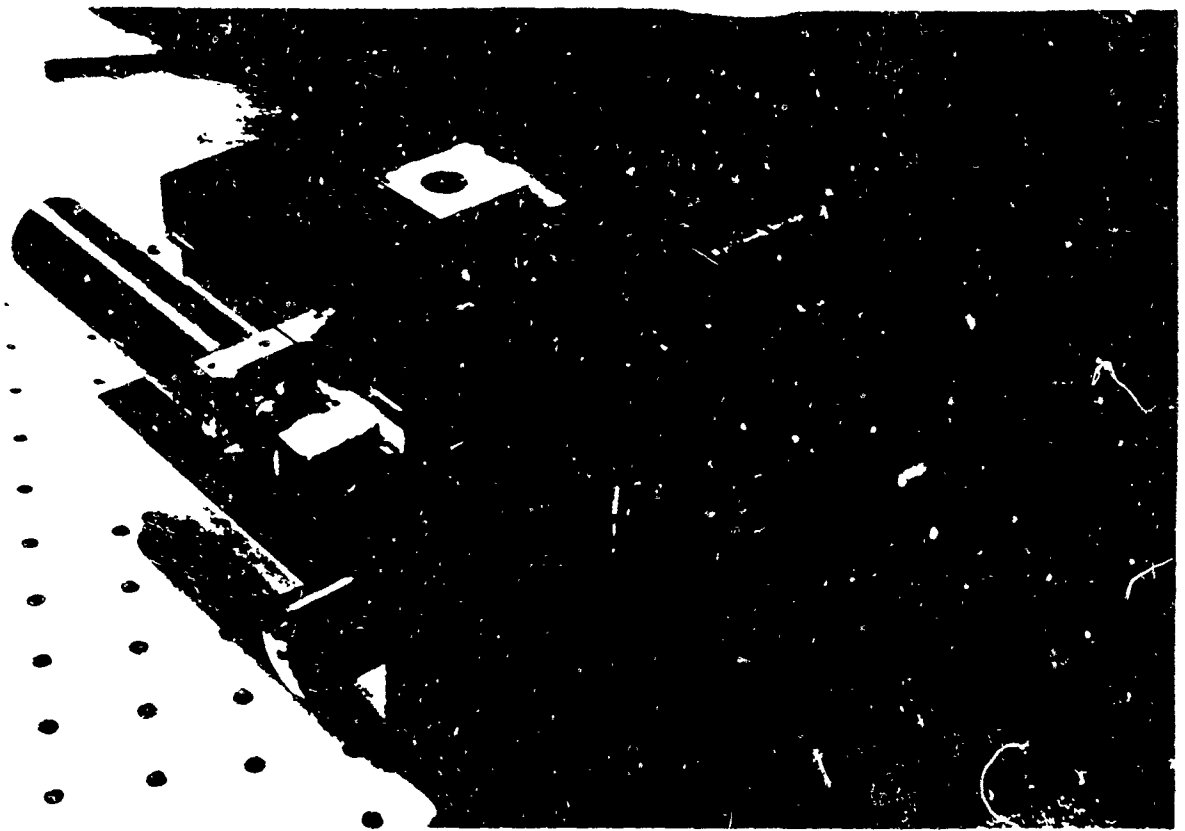


Figure 6

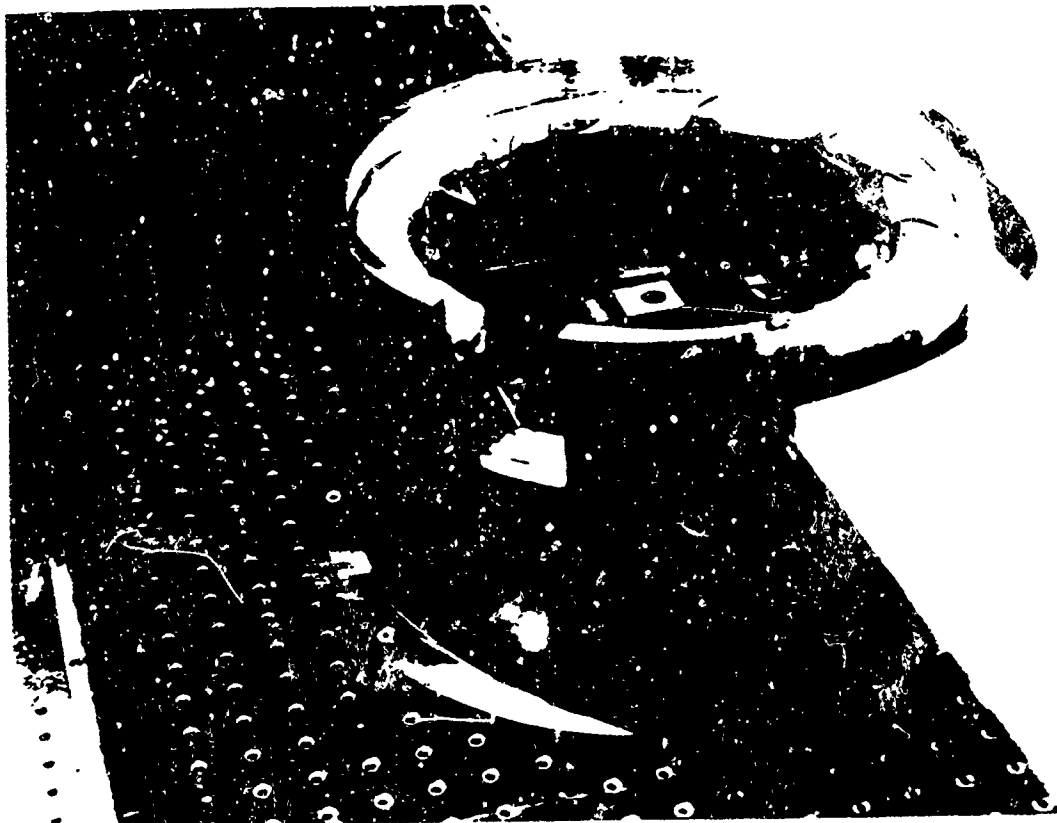


Figure 7



Figure 8



Figure 9

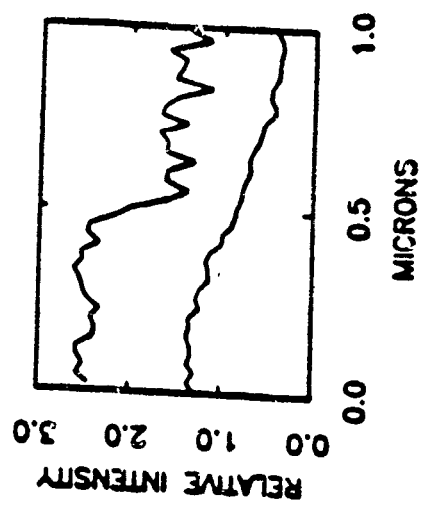


Figure 10

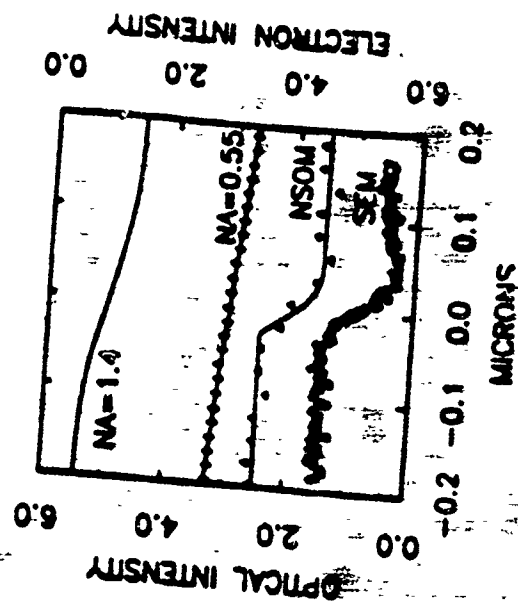


Figure 11

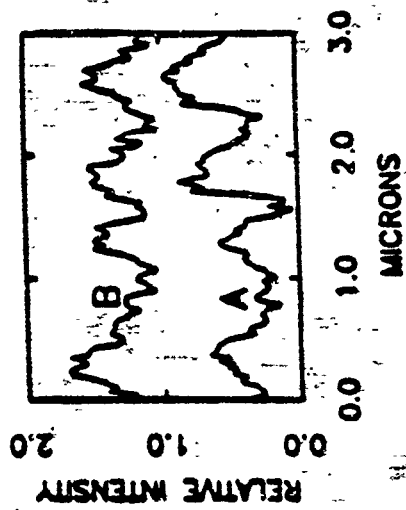


Fig. 12

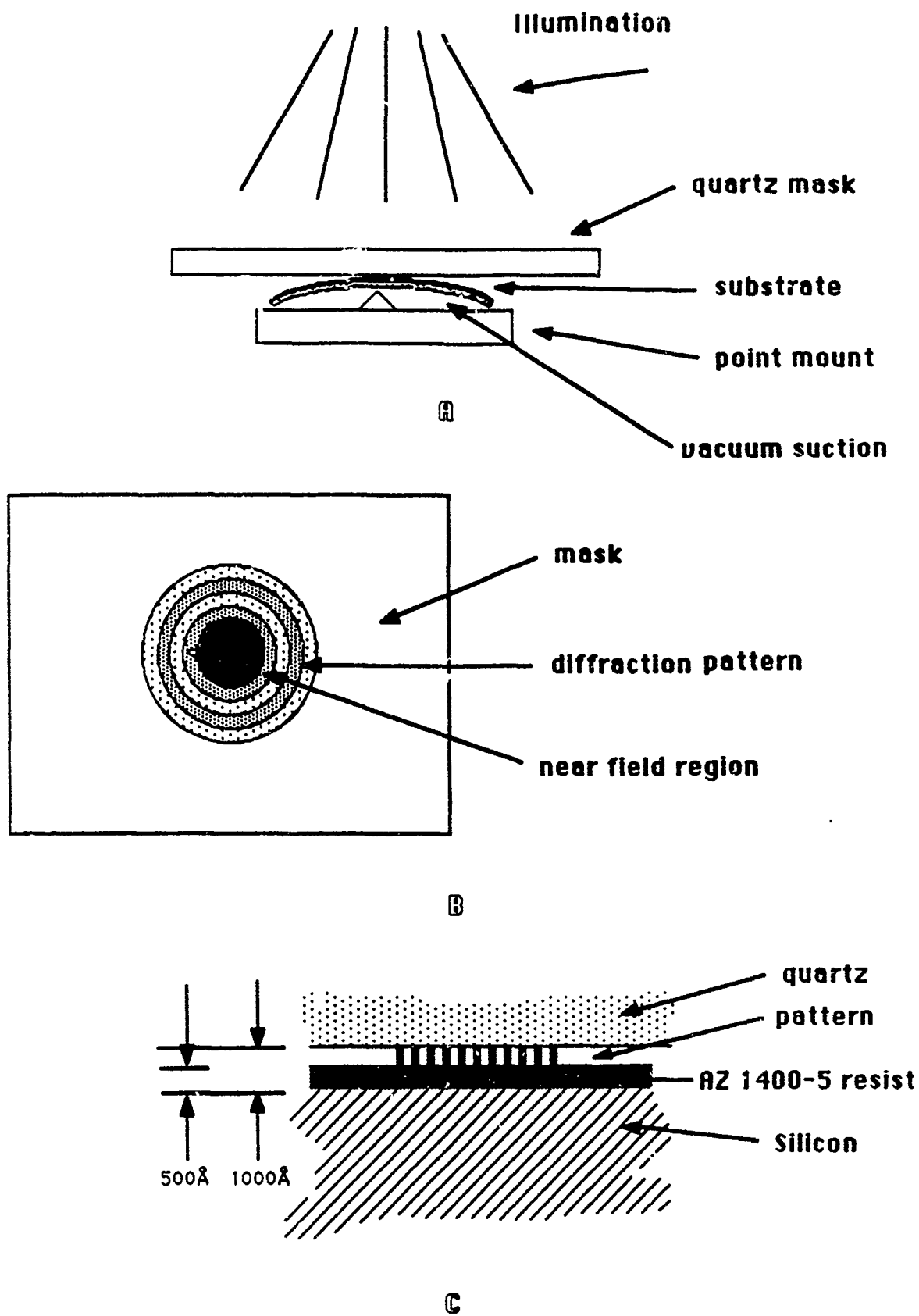


Figure 13

25

side view

top view



A 1000 $\mu$  Si Nitride window is mounted on Si



A layer of PMMA is added

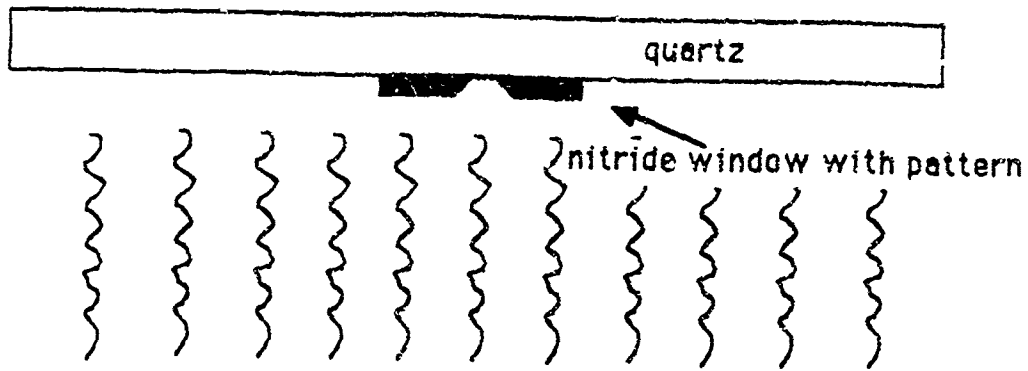


Pattern is exposed with E beam and developed

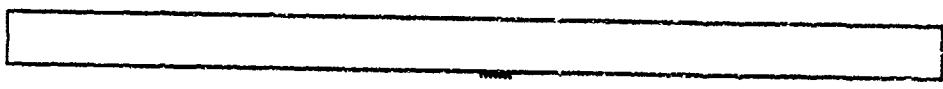


Pattern is etched through Si nitride window

Figure 14



Thermal evaporation of Cr or Al (500 Å)



quartz mask with Cr or Al pattern

Figure 15

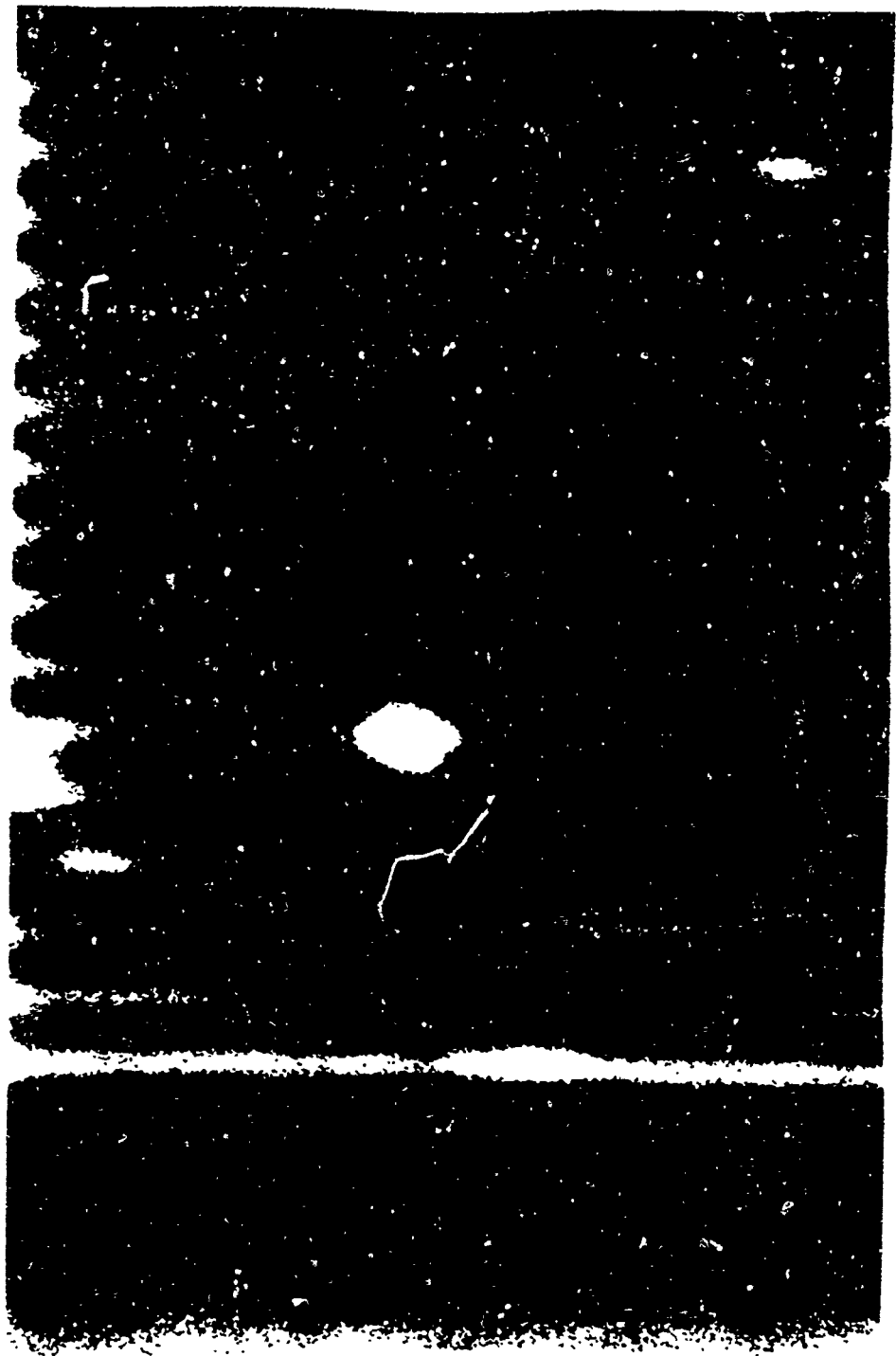
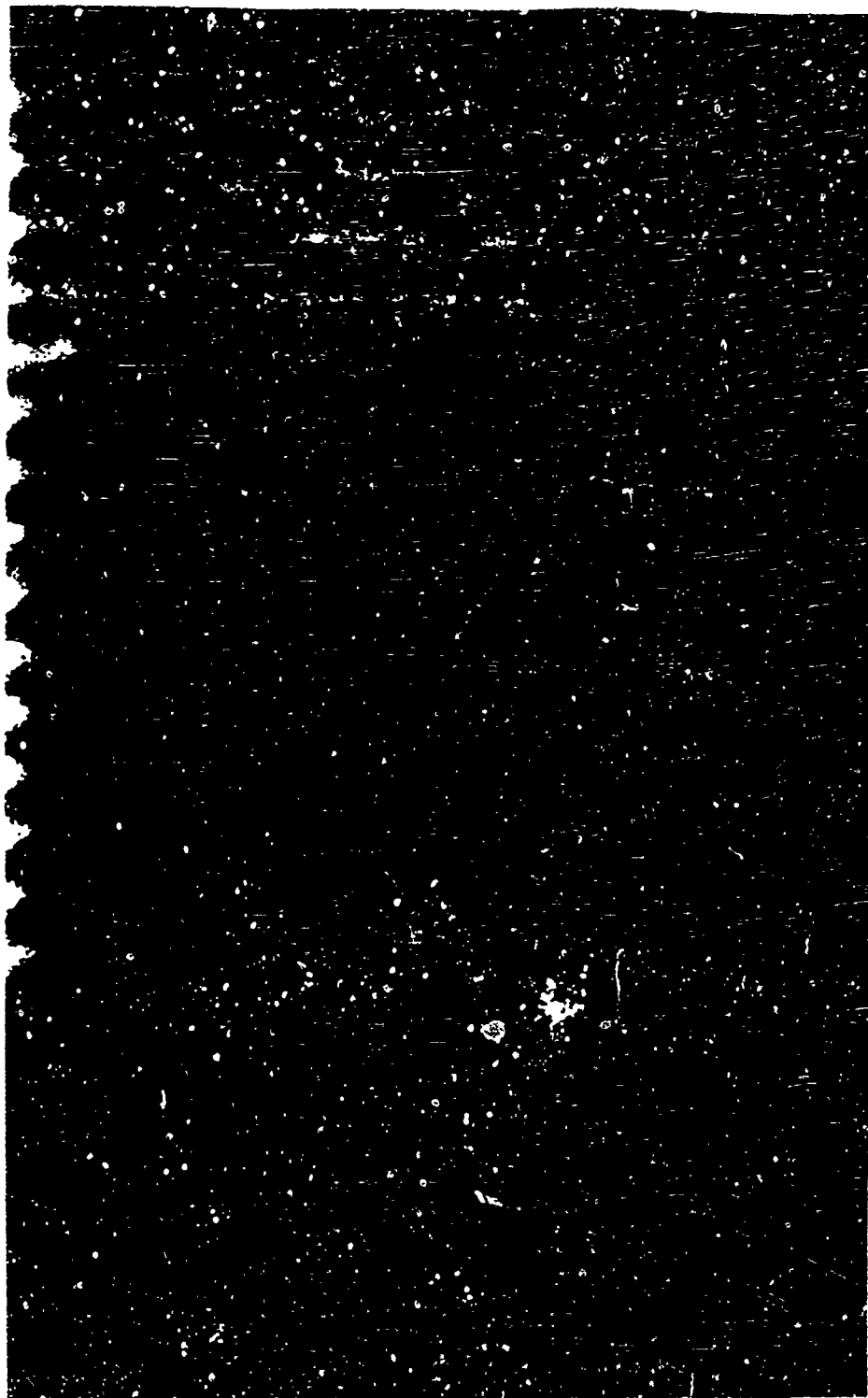


Figure 16



1000 nm

Figure 17